Stability of oxygen point defects in UO_2 by first-principles DFT$+U$ calculations: Occupation matrix control and Jahn-Teller distortion

Boris Dorado,[1] Gérald Jomard,[2] Michel Freyss,[1] and Marjorie Bertolus[1]

[1]*CEA, DEN, DEC, Centre de Cadarache, 13108, Saint-Paul-lez-Durance, France*
[2]*CEA, DAM, DIF, F-91297 Arpajon, France*

Point-defect formation energies in uranium dioxide UO_2 are still a matter of debate due to the significant discrepancies between the various studies published in the literature. These discrepancies stem from the density functional theory (DFT)$+U$ approximation that creates multiple energy minima and complexifies the search for the ground state. We report here DFT$+U$ values of the formation energies for the single oxygen interstitial and vacancy in UO_2, both in the fluorite and the Jahn-Teller distorted structures, using a scheme developed on bulk UO_2 [B. Dorado, B. Amadon, M. Freyss, and M. Bertolus, Phys. Rev. B **79**, 235125 (2009)] and based on occupation matrix control. We first investigate the Jahn-Teller distortion in UO_2 in the noncollinear antiferromagnetic order and we show that the distortion stabilizes the system by 50 meV$/UO_2$ compared to the fluorite structure. Moreover, it is found that the oxygen atoms are displaced in the $\langle 111 \rangle$ directions, in agreement with experiments. For the bulk fluorite structure, we show that the use of the Dudarev approach of the DFT$+U$ without occupation matrix control systematically yields the first metastable state, located 45 meV$/UO_2$ above the ground state. As a result, all previously published point-defect formation energies are largely underestimated. We then use the occupation matrix control scheme to calculate the formation energies of the single oxygen interstitial and vacancy in UO_2. We confirm that this scheme always allows one to reach the lowest energy states and therefore yields reliable formation energies. Finally, we compare our values with those obtained in previous studies and show that the discrepancies observed stem from the calculations of defective supercells which have reached different metastable states.

I. INTRODUCTION

The failure of standard approximations of the density-functional theory[1,2] to describe strongly correlated materials, such as actinide compounds, has led to the development of new approximations, in particular, hybrid functionals,[3] self-interaction correction[4] or the density functional theory (DFT)$+U$ formalism.[5] Uranium dioxide (UO_2) is the conventional fuel of current nuclear reactors and has been in recent years extensively studied using the DFT$+U$ formalism. In particular, the stability of oxygen and uranium point defects,[6–13] as well as the solubility of fission products[12,14–18] in this material were investigated. Such studies are of prime importance to better understand the behavior of UO_2 under irradiation. Resulting formation and solution energies can be used as input data in higher scale models and should therefore be calculated with high accuracy. Unfortunately, significant discrepancies have been observed in the formation energies of point defects calculated at the DFT$+U$ level and published so far, although the same method [projector augmented-wave (PAW) method] and very similar calculation parameters were used. As shown in a previous study on the perfect UO_2 crystal,[19] these discrepancies stem from the use of the DFT$+U$ approximation. This formalism localizes electrons and creates numerous local-energy minima,[20–23] or metastable states, which makes it difficult to find the ground state of the system. This increased number of energy minima has also been observed in UO_2 within other approximations that localize electrons, such as hybrid functionals,[3,24] as well as in other compounds such as Ce,[22] PuO_2,[23] or PrO_2.[25]

In our previous study,[19] we have shown that if one wishes to reach the ground state systematically, the most effective method is to switch off all wave-function symmetries and to control the electronic occupancies of the $5f$ orbitals, i.e., to impose initial occupation matrices (OMs) and monitor them during the calculations. The present study is the application of this method to large defective supercells. Our objective is to obtain the most reliable formation energies of point defects in UO_2 within the DFT$+U$ approximation. For this purpose, we assess the accuracy of the method developed to calculate formation energies of two oxygen point defects in UO_2 (interstitial and vacancy).

All the authors[6,7,10,12–15] who studied point defects and fission products in UO_2 within the DFT$+U$ approximation used the Dudarev approach as implemented in the VASP code.[26–28] Consequently, in order to get further insight into the discrepancies observed in the formation energies, we have implemented the possibility to control the occupation matrices in VASP, namely, by allowing one to define initial electronic occupancies. Using this method, we have then studied the stability of the Jahn-Teller (JT) distortion in UO_2 and calculated point-defect formation energies in both the fluorite and the Jahn-Teller distorted structures. This is the first study of the Jahn-Teller distortion in UO_2 within the PAW formalism.[29,30]

The paper is organized as follows: in Sec. II, we present the computational details and recall briefly the DFT$+U$ formalism. In Sec. III, we study the stability of the Jahn-Teller distortion in bulk UO_2, as well as the influence of the antiferromagnetic ordering, after validating our occupation matrix control implementation. In Sec. IV, we calculate the formation energies of the single-oxygen interstitial and vacancy in the two UO_2 phases (fluorite and Jahn-Teller distorted

phases). Finally, in Sec. V, we compare our results with the ones from the literature and discuss the discrepancies observed.

II. COMPUTATIONAL DETAILS

All calculations presented here were carried out in the PAW formalism[29,30] and using the VASP code.[26–28] Given the failure of standard density functionals [local-density approximation (LDA) and generalized gradient approximation (GGA)] to describe uranium dioxide, we used the DFT+U approximation which improves the treatment of the correlations between uranium $5f$ electrons. The DFT+U energy functional is given by

$$E_{\text{DFT}+U} = E_{\text{DFT}} + E_{\text{Hub}} - E_{\text{dc}} \quad (1)$$

where E_{DFT} is LDA or GGA contribution to the energy, E_{Hub} the electron-electron interactions from the Hubbard term, and E_{dc} the double-counting correction. The DFT+U approximation is thus a correction to the standard DFT energy functional. E_{Hub} and E_{dc} depend on the occupation matrices of the correlated orbitals. We used the two currently available approximations for the Hubbard term E_{Hub}: the rotationally invariant version introduced by Liechtenstein *et al.*[31] and the simplified rotationally invariant approach due to Dudarev *et al.*[5] As regards the double counting correction, we used the local spin density approximation (LSDA) +U formulation, also called the fully localized limit,[31] whose expression is

$$E_{\text{dc}} = \frac{U}{2}N(N-1) - \frac{J}{2}\sum_\sigma N^\sigma(N^\sigma - 1). \quad (2)$$

For the exchange and correlation energy, we used the GGA functional as parametrized by Perdew, Burke, and Ernzerhof (PBE).[32]

For the calculations on bulk UO_2, we used a six-atom and a 12-atom cell and studied both the 1**k** (collinear) and the 3**k** (noncollinear) antiferromagnetic (AFM) orders. This allows us to assess the relative stability of the two configurations and thus to validate the approximated collinear order. A 600 eV cut-off energy for the plane-wave basis set was used in these calculations with a $6 \times 6 \times 6$ Monkhorst-Pack[33] k-point mesh for the sampling of the irreducible part of the Brillouin zone.

The perfect UO_2 crystal was represented by a 96-atom supercell with an approximated 1**k** order. We added or removed an oxygen atom from this supercell to create either an interstitial or a vacancy. This leads to an oxygen/metal ratio equal to 2.031 and 1.969, respectively, with a deviation from stoichiometry $x=0.031$. Convergence studies were carried out in order to determine the influence of the cut-off energy in point-defect calculations. The results listed in Table I show that a 500 eV cut-off energy is necessary to obtain converged structural parameters. Absolute total energies, however, are only converged to approximately 24 meV/atom, but we used this cut-off energy to allow for acceptable computational time. The single-oxygen interstitial and vacancy induce a cell volume variation of 0.3% and 0.02%, respectively. We can therefore consider that the supercell size is

TABLE I. Convergence of total energies and structural parameters (a, b and c) with respect to the cut-off energy. The reference energy is taken to be the total energy calculated at 700 eV.

Cut-off energy (eV)	$E - E_{700}$ (meV/atom)	a, b (Å)	c (Å)
400	27	5.502	5.517
500	24	5.536	5.553
600	8	5.537	5.552
700	0	5.538	5.554

large enough to accommodate these defects. A $2 \times 2 \times 2$ k-point mesh, yielding four k points in the irreducible part of the Brillouin zone, is sufficient to get converged structural parameters and total energies. The defective supercell volume is kept constant during the calculations and equals the perfect supercell volume.

For all calculations, the U and J parameters of the DFT +U approximation were set to 4.50 eV and 0.51 eV, respectively, as determined by Kotani and Yamazaki,[34] based on the analysis of x-ray photoemission spectra. Finally, we used a Gaussian smearing for fractional occupancies with a smearing width of 0.1 eV.

As mentioned above, we implemented the possibility of defining initial occupation matrices and impose them during the calculation of the DFT+U potential in the VASP code. We thus precondition the calculation of the potential which is then applied as a correction to the standard DFT potential. Occupation matrices are imposed during the first ten electronic steps. After these ten steps, the constraint is lifted and the calculation is left to converge self-consistently on its own.

III. BULK URANIUM DIOXIDE

Our previous work[19] showed that in order to reach the ground state of UO_2 using the DFT+U approximation, it was necessary to switch off all symmetries and to control the $5f$ electronic occupancies, i.e., to define initial occupation matrices, impose them during the first electronic steps and monitor them during the calculations. As symmetries are lowered, the degeneracies of orbitals are lifted and electrons have more freedom to find lower states. This is all the more necessary in UO_2 since it has been shown experimentally that this material exhibits at low temperature a Jahn-Teller distortion of the oxygen cage.[35–39] We did not, however, consider the Jahn-Teller distortion in our work in Ref. 19 and we obtained the ground state of the fluorite structure. The aim of this section is to investigate the stability of the Jahn-Teller distorted UO_2 with respect to the fluorite structure, as well as the influence of the magnetic ordering. For this purpose, we first validate our implementation of occupation matrix control in VASP by comparing results with those obtained in Ref. 19. We also compare the results on UO_2 given by the Liechtenstein and the Dudarev approaches of the DFT+U.

A. Fluorite $Fm\bar{3}m$ structure

1. Liechtenstein's approach

In these calculations, we model UO_2 in its ideal fluorite

TABLE II. Relative energies of the states obtained starting from the 21 initial diagonal occupation matrices, calculated with the Liechtenstein DFT+U. E_{GS} is the total energy of the ground state.

i	j	Matrix	$E-E_{GS}$ (this work) (eV/U$_2$O$_4$)	$E-E_{GS}$ (Ref. 19) (eV/U$_2$O$_4$)	Comment
−3	−2	[1100000]			No convergence
−3	−1	[1010000]	0.06	0.02	First metastable state
−3	0	[1001000]	1.81	1.89	Metallic
−3	1	[1000100]	0.06	0.74	Different states
−3	2	[1000010]	1.66	1.65	Metallic
−3	3	[1000001]	3.34	3.48	
−2	−1	[0110000]	0.00		Ground state
−2	0	[0101000]	1.53	1.67	
−2	1	[0100100]	0.00		Ground state
−2	2	[0100010]	2.19	2.64	
−2	3	[0100001]			No convergence
−1	0	[0011000]	1.81	1.89	Metallic
−1	1	[0010100]	0.81	0.74	
−1	2	[0010010]	2.06	1.65	Metallic
−1	3	[0010001]	0.06	0.02	First metastable state
0	1	[0001100]	1.81	1.89	Metallic
0	2	[0001010]	0.18	0.12	
0	3	[0001001]	1.81	1.89	Metallic
1	2	[0000110]	2.00	1.65	Metallic
1	3	[0000101]	0.06	0.02	First metastable state
2	3	[0000011]	1.66	2.34	Different metallic states

structure (space group: $Fm\bar{3}m$) and the wave-function symmetries are taken into account. Using the Liechtenstein approach, we perform a similar systematic study as that of Ref. 19 on a six-atom UO$_2$ primitive cell: we study the states reached by the calculation depending on the initial electronic occupancies. In order to span the entire potential-energy surface, we should have imposed numerous diagonal and nondiagonal occupation matrices. To validate our implementation, however, diagonal occupation matrices are sufficient. We recall that there are 21 possible diagonal occupation matrices which correspond to the 21 different ways of filling the seven $5f$ orbitals with the two electrons of the U^{4+} uranium cation. The relative energies of the states obtained from the 21 diagonal occupation matrices (using the simplified notation introduced in Ref. 19) are presented in Table II.

We see that the results obtained in our work are very close to those presented in Ref. 19: there are ten different states and the insulating or metallic character of these states is well reproduced. It can also be seen that the differences in energy between metastable states are very similar in the two studies. Finally, the occupation matrices obtained are also in perfect agreement. Their expression is given in Appendix. It should first be noted that these occupation matrices only differ by the signs of the nondiagonal terms in the spin ↑ component. Then, as we did not take into account the spin-orbit coupling, there is no off-diagonal spin component (↑↓ or ↓↑ component) and the occupation matrices hence predict no orbital magnetic moment.

A few differences, however, are observed between the two studies. First, we see that in the present study, two of the 21 initial diagonal occupation matrices allow us to reach the ground state ([0110000] and [0100100]). These two occupation matrices are identical by symmetry and it is therefore consistent that they both lead to the same state. In Ref. 19, the calculations starting from these two occupation matrices did not converge and imposing only diagonal occupation matrices did not allow us to reach the ground state. Second, some initial occupation matrices (namely, [1000100] and [0000011]) do not lead to the same final state in the two studies. These differences probably stem from the fact that the various energy minima are very close to each other and that two different electronic minimization algorithms were used in the two studies. Another difference is that the first metastable state lies 63 meV above the ground state in the present study. This energy difference is significantly larger than the value found previously (23 meV). This could be due to the difference in the PAW atomic data sets used for uranium and, in particular, in the PAW cut-off radius, which affect the electronic occupancies obtained.

These results therefore enable us to validate our implementation of occupation matrix control in the VASP code. We now switch to the Dudarev approach of the DFT+U, since it is the most widely used approach in studies of uranium dioxide and its defects available in the literature. This will allow us to compare directly our results with those already published and make a comparison between the Liechtenstein and Dudarev approach of the DFT+U.

TABLE III. States of bulk uranium dioxide U_2O_4 reached depending on the initial imposed OM. The Dudarev DFT+U is used. Metastable states are sorted by increasing relative energy (ΔE) with respect to the ground state.

State	Initially imposed OM	ΔE (meV/U_2O_4)
GS	Liechtenstein first MS	0
MS_1	Liechtenstein GS	87
MS_2	[0001010]	249
MS_3	[0010100]	701
MS_4	[0010010]	1256
MS_5	[0100010]	1301
MS_6	[0101000]	1601
MS_7	[1001000]	1678
MS_8	[1000001]	1722
MS_9	[1000010]	1995
MS_{10}	[0011000]	2317
MS_{11}	[1010000]	2996
MS_{12}	[1100000]	3315

2. Dudarev's approach

We still consider the ideal fluorite structure and take all symmetries into account. We impose the 21 possible diagonal occupation matrices, as well as numerous nondiagonal occupation matrices, in particular, the occupation matrices of the Liechtenstein ground state and first metastable state that were determined in Sec. III A 1. We then sort the metastable states obtained according to their relative energy with respect to the ground state. Results are presented in Table III.

It is observed that the first metastable state lies 87 meV above the ground state. This difference in energy between the two states is slightly larger than the value yielded by the Liechtenstein approach (63 meV). We also see that the Dudarev ground state is the Liechtenstein first metastable state and vice versa. For the fluorite structure, the Dudarev ground-state occupation matrices will be used in Sec. IV for the calculations of point-defect formation energies and will be referred to as OM_F (F for Fluorite). The fact that the UO_2 ground state depends on the DFT+U formalism shows that the physical meaning of the first two states is unclear and that only a method which allows fluctuations between states [such as LDA+dynamical mean field theory (DMFT)] (Refs. 40 and 41) may improve the system electronic description.

It should also be stressed that the two DFT+U approaches yield very similar electronic states. This is consistent since the Dudarev approach is a simplified version of the Liechtenstein approach. The states reached are structurally identical with the exact same cell parameters. The occupation matrices are, however, slightly different. Though having the same form (same as given in Appendix), the electronic occupancies differ. This is one of the reason why we observe a total-energy difference of 0.25 eV/UO_2 between the two DFT+U functionals.

Moreover, we found that the state reached when electronic occupancies are not controlled is the Liechtenstein

TABLE IV. Total energies of bulk $U_{32}O_{64}$ calculated using the Dudarev approach with and without imposing occupation matrices. The error made by considering the fluorite structure without occupation matrix control is also presented. Some symmetries are taken into account.

Cut-off energy (eV)	Imposed occupation matrices	Total energy (eV/$U_{32}O_{64}$)	Error (eV)
400	OM_F	−930.248109	
400	None	−928.759564	1.49
500	OM_F	−930.560748	
500	None	−929.032588	1.53
600	OM_F	−932.053732	
600	None	−930.516873	1.54

ground state. As the two DFT+U approaches switch the first two states, it means that without occupation matrix control, the Dudarev approach always reaches the first metastable state. As mentioned above, this metastable state lies 87 meV above the ground state. Its presence thus induces an error in the total energy of about 45 meV per uranium atom, which becomes significant in the case of 96-atom supercells used in the defect study. A first estimate of the error on the total energy of these supercells is 1.4 eV.

In order to confirm this estimate, we calculated the total energies of the perfect 96-atom supercell in the Dudarev approach using symmetries, both in the ground state (i.e., imposing the OM_F matrix) and the first metastable state (i.e., leaving the calculation converge on its own). To check the influence of the cut-off energy on the total energy, we used three different cut-off energies: 400, 500, and 600 eV. Results are presented in Table IV.

Several conclusions can be reached from these results. First, the total energies obtained are always lower when occupation matrices are controlled. As mentioned previously, letting the calculation converge on its own always yields the first metastable state of the fluorite structure. Second, as expected, reaching the first metastable state leads to an error in the total energy of the supercell of approximately 1.5 eV. This error is almost independent of the cut-off energy. Finally, it should be noted that the structural parameters depend on the state obtained. In the Dudarev approach, the ground state exhibits a c parameter slightly larger than a and b ($c/a > 1$). This slight dilatation occurs along the c axis because of the approximated 1**k** AFM order considered.[19] On the contrary, the first metastable state exhibits a c parameter slightly smaller than a and b ($c/a < 1$). This constitutes a simple test to check whether the ground state of the fluorite structure has been reached in a calculation.

B. Breaking the $Fm\bar{3}m$ symmetry: The Jahn-Teller distortion in UO_2

It has been shown experimentally that UO_2 exhibits at low temperature a Jahn-Teller distortion of the oxygen cage.[35–39] Without this distortion UO_2 would have a degenerate ground state: in the paramagnetic fluorite structure, the point-group
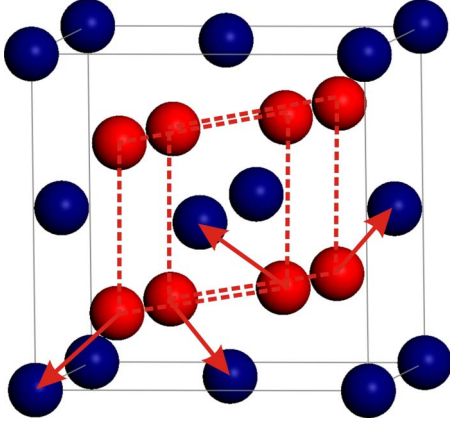
FIG. 1. (Color online) Jahn-Teller distortion of uranium dioxide as observed experimentally. The displacement of oxygen atoms (represented by arrows) were multiplied by ten in order to make the distortion of the oxygen cage visible.

symmetry of uranium atoms is O$_h$ and the crystal field splits the seven $5f$ orbitals into two threefold degenerate T$_{1u}$ and T$_{2u}$ levels and a nondegenerate A$_{2u}$ level. The two electrons of the U^{4+} cations must therefore be placed in the lowest threefold degenerate level, which results in three possible configurations. The distortion of the oxygen cage enables the crystal to lift this degeneracy, hence the Jahn-Teller denomination. Experimentally, the oxygen cage is distorted with a displacement of oxygen atoms of 0.014 Å in the $\langle 111 \rangle$ directions (Fig. 1), changing the space group from $Fm\bar{3}m$ to $Pa\bar{3}$.[39]

The Jahn-Teller distortion is in UO$_2$ directly linked to the orientation of the magnetic moments of uranium atoms. Experimentally, UO$_2$ exhibits a noncollinear (3**k**) AFM order[39] with uranium magnetic moments pointing toward the $\langle 111 \rangle$ directions. This noncollinear AFM order is difficult to model and is commonly approximated by a collinear (1**k**) AFM order. In this section, we first perform calculations to investigate the stability of the Jahn-Teller distortion in UO$_2$, in the 1**k** order. Then, we assess the validity of the 1**k** approximation by comparing its total energy to the 3**k** structure. The spin-orbit coupling is neglected in these calculations but its effect will be briefly discussed in Sec. III B 2.

1. Stability of the Jahn-Teller distortion in the 1k order

We first consider the 1**k** order in which uranium atoms have magnetic moments which change sign along one particular axis (in our case, the c axis). Calculations are performed in a 12-atom unit cell starting from the Jahn-Teller distorted structure without taking symmetries into account. The total energy of the 1**k** Jahn-Teller distorted structure is then compared with the one obtained in the 1**k** fluorite structure, in its ground state (Sec. III A 2).

Table V shows that the Jahn-Teller distortion stabilizes the structure by 50 meV/UO$_2$. This is significant since in a 96-atom supercell it would decrease the total energy of the perfect crystal by approximately 1.6 eV/U$_{32}$O$_{64}$. Additional calculations were performed in the Jahn-Teller distorted phase with several different initial occupation matrices.

TABLE V. Stability of the Jahn-Teller distortion in the 1**k** AFM UO$_2$ with respect to the fluorite structure within the Dudarev DFT$+U$.

Structure	Space group	Total energy (eV)	$E-E_{min}$ (meV/UO$_2$)
Fluorite	$Fm\bar{3}m$	−116.505199	51.8
Jahn-Teller	$Pa\bar{3}$	−116.712499	

Since all calculations yielded the same final state, it is very likely that the ground state has been reached for this structure. This confirms that breaking the $Fm\bar{3}m$ symmetry by atomic displacements facilitates the search for the ground state, as shown in our previous study.

The oxygen-cage distortion, however, does not occur in the $\langle 111 \rangle$ directions, as seen experimentally. This is due to the approximated 1**k** order considered since, as mentioned above, the distortion is closely related to the magnetic moments of uranium atoms. These are, however, the first DFT $+U$ calculations in the PAW formalism yielding the Jahn-Teller distorted structure as the most stable phase of UO$_2$.

In this Jahn-Teller distorted structure, all uranium atoms have similar occupation matrices which only differ by the signs of several terms. These occupation matrices will be used in Sec. IV for the calculation of point-defect formation energies and will be referred to as OM$_{JT}$ (JT for Jahn-Teller). Calculation results also point out that in the perfect crystal, occupation matrices depend on the oxygen positions in the supercell. This is because the oxygen atoms govern the crystal field applied on the uranium atoms. In the 1**k** fluorite structure, the point-group symmetry of uranium atoms is D$_{4h}$ and the crystal field imposes a particular form to the occupation matrices. If the oxygen cage is distorted, however, the point-group symmetry is then C$_{3i}$ and the occupation matrices exhibit a different form. Reciprocally, the initial occupation matrices govern the final positions of the oxygen atoms. We performed a calculation in the $Fm\bar{3}m$ symmetry and imposed occupation matrices corresponding to the Jahn-Teller distorted structure (OM$_{JT}$). We then saw that the oxygen atoms move from their fluorite to their Jahn-Teller positions and that the final total energy is very close to the energy of the Jahn-Teller distorted structure.

2. Stability of the 3k order in UO$_2$

As mentioned above, the 1**k** order is an approximation of the 3**k** order observed experimentally[39] in which the uranium magnetic moments point toward different $\langle 111 \rangle$ directions. In order to determine exactly the error caused by this approximation, we compared the total energies of the 1**k** and the 3**k** structures. We used a 12-atom primitive cell, which is the minimum cell size required to reproduce the 3**k** order. There are four uranium atoms in the cell. Their fractional coordinates and their magnetic moments are presented in Table VI. Calculations were performed starting from the experimental Jahn-Teller distortion. Both atomic positions and cell volume were optimized and symmetries were switched off. The final total energies are presented in Table VII.

TABLE VI. Magnetic moments of the uranium atoms in a 12-atom conventional cell exhibiting a 3**k** AFM order.

Fractional coordinates	Magnetic moments
(0.00,0.00,0.00)	(1.2, 1.2, 1.2)
(0.50,0.50,0.00)	(1.2, −1.2, −1.2)
(0.50,0.00,0.50)	(−1.2, −1.2, 1.2)
(0.00,0.50,0.50)	(−1.2, 1.2, −1.2)

We see that the two structures have similar total energies. The 1**k** order is, however, slightly more stable than the 3**k** order, contrary to what is observed experimentally. This order of stability might change with the inclusion of the spin-orbit coupling in the calculations. It would indeed yield drastic changes in the occupation matrices due to the filling of complex spherical harmonics that would give rise to large matrix elements in the nondiagonal ↑↓ and ↓↑ spin components. We have performed several calculations including the spin-orbit coupling in order to calculate the orbital magnetic moment of uranium atoms in the fluorite phase of UO_2. We find it to be equal to $\pm 3.3\mu_B$ per uranium atom, which compares well to the value found by Dudarev *et al.*[42] and Laskowski *et al.*[43] The occupation matrices yielded by these calculations indeed display large complex off-diagonal elements. Such changes in the occupation matrices, however, require a new systematic search for the ground state, which is not in the scope of this study where we study defect formation energies that can be compared with other values reported in the literature where spin-orbit coupling was neglected.

Finally, it is seen that in the 3**k** AFM structure, the cell is perfectly cubic ($a = b = c$) and the oxygen cage undergoes a distortion Δ_O of 0.09 Å in the $\langle 111 \rangle$ directions, which is significantly larger than the distortion observed experimentally. Our results are, however, consistent with the all-electron calculations performed by Laskowski *et al.*,[43] who also calculated the 1**k** structure to be most stable, as well as a large distortion of the oxygen cage ($\Delta_O = 0.16$ Å).

The above results emphasize that the 1**k** order is a good approximation of the 3**k** order and therefore justifies its use in our calculations of point-defect formation energies. As the Jahn-Teller distorted structure is found to be the most stable phase, we will calculate formation energies in both phases of UO_2.

IV. STABILITY OF $UO_{2\pm x}$

This section reports the values of the formation energies of the single-oxygen interstitial and vacancy in UO_2 calcu-

TABLE VII. Relative stability and cell parameters of the 12-atom primitive cell in 1**k** and 3**k** AFM orders without the spin-orbit coupling.

	1**k** order	3**k** order
Total energy (eV)	−116.712526	−116.710061
$E_{3k} − E_{1k}$ (meV/UO_2)	0	0.61
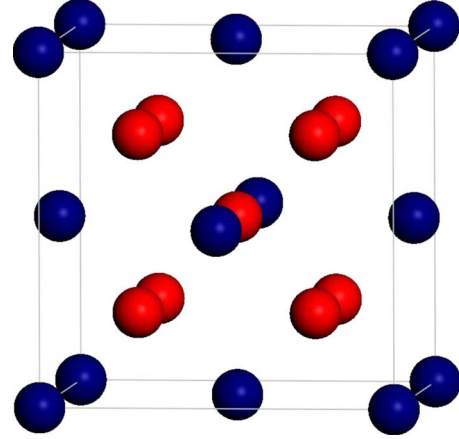
FIG. 2. (Color online) Local environment of a single oxygen atom in an octahedral interstitial site (the center of the cube). Blue atoms stands for uranium atoms while red atoms stand for oxygen atoms.

lated with occupation matrix control. It should be stressed that the formation energies calculated for the Jahn-Teller distorted structure cannot be directly compared with experimental data at ambient or higher temperature since it is only stable below 30 K. Consequently, we also studied the case of the fluorite structure for comparison with experimental data. To calculate formation energies in the fluorite structure, however, several adequate wave-function symmetries were kept in order to prevent the system from getting back to the most stable phase, i.e., the Jahn-Teller distorted phase. For the investigation of the oxygen interstitial, the extra oxygen atom is added in a 96-atom supercell at an octahedral interstitial site (see Fig. 2). It exhibits six uranium atoms as first-nearest neighbors (located at the center of the faces) and eight uranium atoms as second-nearest neighbors (located at the corners of the cube). In this configuration ($U_{32}O_{65}$), the oxygen/metal (O/M) ratio equals 2.031. The oxygen vacancy is surrounded by four uranium atoms as first-nearest neighbors and the O/M ratio equals 1.969.

Our objective is to provide the most reliable point-defect formation energies in the fluorite and Jahn-Teller distorted phases in checking the ground state is reached or approached as much as possible in the calculations of defective supercells. The search for the ground state in large defective supercells is even more complex than in perfect crystal structures and we show how occupation matrix control can prevent the system from being trapped in metastable states. For this purpose, we performed calculations in both phases with occupation matrix control, as well as default calculations for comparison. We also used as initial wave functions those obtained in a preliminary spin-polarized GGA (SP-GGA) calculation, as has been done in Refs. 12 and 24.

A. Hyperstoichiometric UO_{2+x}

The formation energy of the single-oxygen interstitial is given by

TABLE VIII. Relative energies of the Jahn-Teller distorted structure containing an oxygen interstitial, starting from different electronic occupancies.

Initial OM	$E - E_{\min}$ (eV)
Default	0.32
OM$_{JT}$	0.00
SP-GGA calculation	0.04

$$E_{I_O}^F = E_{I_O}^{97} - E^{96} - \frac{1}{2}E_{O_2}, \tag{3}$$

where $E_{I_O}^{97}$ is the total energy of the supercell with the single-oxygen interstitial, E^{96} is the total energy of the perfect supercell in its ground state (i.e., either the fluorite or the Jahn-Teller distorted structure), and E_{O_2} is the total energy of the reference state of oxygen: the dioxygen molecule O$_2$ in its triplet state calculated using the spin-polarized GGA approximation. For the dioxygen molecule, we find the binding energy to be 30% higher than the experimental value. The larger part of this error (2/3) comes from the limitation of the PBE functional to describe the O$_2$ molecule.[32] The rest of the error is probably due to the PAW data set of the oxygen atom. It is difficult, however, to tell whether it acts on the total energy of the dioxygen molecule or the single oxygen atom. In the latter case, the error would have no influence on the calculated formation energies.

Table VIII shows the result of the three calculations performed on the Jahn-Teller distorted structures. It can be seen that the lowest energy state was obtained when the occupation matrix control scheme was used. Furthermore, one should notice that the three different calculations lead to three different results, which is the origin of the discrepancies observed in the literature, as will be discussed in Sec. V. Thanks to occupation matrix control, uranium atoms far from the defect and which are not affected by its presence are in their ground state. It should also be stressed that in the lowest state, oxygen atoms did not move back to their ideal fluorite positions. The most stable phase is thus a Jahn-Teller distorted structure. Furthermore, starting from SP-GGA wave functions is also an effective way of approaching the system ground state. This particular scheme was used in our previous study of the incorporation of iodine in UO$_2$.[12] The highest energy states are obtained using the default calculations without occupation matrix control, both in $Fm\bar{3}m$ and $Pa\bar{3}$ structures.

Table IX presents the formation energies $E_{I_O}^F$ of the oxygen interstitial in the fluorite and the Jahn-Teller distorted

TABLE IX. Formation energies of the single-oxygen interstitial and vacancy in the fluorite and the Jahn-Teller distorted structures.

Structure	$E_{I_O}^F$	$E_{V_O}^F$
Fluorite (with OM$_F$)	0.10	5.67
Jahn-Teller distortion (with OM$_{JT}$)	0.47	6.01

structures. It can be seen that the formation energies are positive in both phases, 0.10 eV and 0.47 eV, respectively. The formation energy in the Jahn-Teller distorted structure is therefore 0.37 eV larger than the one in the fluorite structure. Both these energies are small and the question of the sign of the oxygen interstitial formation energy is still a matter of debate. It seems consistent, however, to find a positive formation energy for the Jahn-Teller distorted UO$_{2+x}$ given that this hyperstoichiometric phase is not stable at 0 K.[44]

In both the fluorite and Jahn-Teller distorted phases, we observed the presence of two U^{5+} cations. We performed several additional calculations to determine their most stable location and found it to be the second coordination sphere of the extra interstitial oxygen atom. The optimal separation distance between the two cations is then $d=9.64$ Å. The magnetic moments of these two cations changed from $\pm 2\mu_B$ to $\pm 1\mu_B$, suggesting the loss of one electron. It should be noted, however, that the presence of the two U^{5+} cations could be an artifact of the DFT$+U$ formalism, which tends to favor integer electronic occupancies.[45] Only an experimental evidence of the presence of U^{5+} ions in UO$_{2+x}$ at low temperature could thus confirm these results.

Finally, we investigated the atomic relaxations of the extra oxygen nearest neighbors. In both the fluorite and the Jahn-Teller distorted structures, the distance between neighboring uranium atoms decreases, resulting in a local decrease in the cell parameters. This is in agreement with experimental observations that the cell parameters decrease with the addition of oxygen in the material. In the work of Teske et al.,[46] they found that the cell parameters decrease as a function of the deviation from stoichiometry x

$$a = (5.4705 - 0.1306x) \tag{4}$$

with a negative slope of 0.1306. We accordingly calculated this slope and found it to be 0.1093 and 0.1132 in the fluorite and the Jahn-Teller distorted structures, respectively. Our calculations are therefore in good agreement with the experimental observations of Teske et al. It can also be seen that the influence of the extra oxygen atom on the cell parameters is similar in the two phases, suggesting that the crystal field does not have a large influence on the defect structural properties.

B. Hypostoichiometric UO$_{2-x}$

The formation energy of the single-oxygen vacancy is given by

$$E_{V_O}^F = E_{V_O}^{95} - E^{96} + \frac{1}{2}E_{O_2}, \tag{5}$$

where $E_{V_O}^{95}$ is the total energy of the supercell with the oxygen vacancy, E^{96} is the total energy of the perfect supercell, and E_{O_2} is the total energy of the dioxygen molecule. We performed the two calculations described above for the fluorite structure and the three calculations for the Jahn-Teller distorted structure.

The results show that the lowest energy states are reached in the Jahn-Teller distorted structure, either with occupation

TABLE X. Formation energy of the unbound oxygen Frenkel pair in the fluorite and the Jahn-Teller distorted structures.

Structure	$E^{\mathrm{F}}_{\mathrm{FP_O}}$
Fluorite (with OM_F)	5.77
Jahn-Teller distortion (with OM_{JT})	6.48

matrix control or when SP-GGA wave functions are used. The fluorite structure states are systematically higher in energy.

Table IX presents the formation energies $E^{\mathrm{F}}_{\mathrm{V_O}}$ of the oxygen vacancy in the two UO_2 phases. It can be seen that the formations energies are similar in the fluorite structure (5.67 eV) and the Jahn-Teller distorted structure (6.01 eV) with a difference of 0.34 eV between the two structures, similar to what was found for the oxygen interstitial. As regards the atomic displacements of the defect nearest neighbors, we found that the oxygen vacancy only triggers slight modifications in the bonding distances (less than 0.05 Å). As a consequence, the cell parameters remains unchanged with and without the defect.

For both oxygen point defects, the above results seem to show that the formation energies in the fluorite are 0.3 to 0.4 eV lower than in the Jahn-Teller distorted structure and that the crystal field in UO_2 has only a moderate influence on the formation energies. Moreover, results show that occupation matrix control gives accurate results because it always allows one to reach the lowest states. Consequently, when calculating defective structures in the DFT+U approximation, one should always control the occupation matrices by imposing the occupation matrices corresponding to the ground state of the phase considered. This is all the more necessary when studying the fluorite structure using the Dudarev approach since its ground state can only be reached by imposing the OM_F occupation matrix.

C. Unbound oxygen Frenkel pair

From the formation energies of the oxygen interstitial and vacancy, we can estimate the formation energy of an unbound oxygen Frenkel pair both in the fluorite and the Jahn-Teller distorted structures. This defect is composed of an interstitial and a vacancy with no interaction between the two defects. It is thus the sum of the two formation energies calculated in this work

$$E^{\mathrm{F}}_{\mathrm{FP_O}} = E^{\mathrm{F}}_{\mathrm{I_O}} + E^{\mathrm{F}}_{\mathrm{V_O}}. \qquad (6)$$

We present in Table X the formation energies of the unbound oxygen Frenkel pair in the fluorite and the Jahn-Teller distorted structures. The Frenkel pair formation energy in the Jahn-Teller distorted structures is much higher than in the fluorite structure. We recall, however, that for comparison with experiments, the fluorite structure should be considered. In this case, the formation energy equals 5.77 eV, which can be compared with the value found in previous DFT+U studies of approximately 4 eV.[6,7,10] Our value is therefore much larger than in the previous studies, due to the larger formation energy found for the oxygen interstitial.

Previous investigations of defects in UO_2 (Refs. 7 and 12) have shown that interactions between defects have a large influence on the formation energies and should then be taken into account in calculations of complex point defects. Formation energies of bound Frenkel pairs should therefore be calculated. This involves supercells containing both the oxygen interstitial and vacancy. However, due to the relatively small size of the supercells which can currently be considered, the oxygen interstitial can only be first- or second-nearest neighbor of the vacancy. In both cases, the oxygen interstitial atom gets back into the vacancy. This result is consistent with the results of a recent classical molecular dynamics study by Van Brutzel *et al.*,[47] where recombination is observed for these two positions of the interstitial oxygen atom.

V. COMPARISON OF OUR RESULTS WITH THOSE OF THE LITERATURE

We showed in Sec. III A 2 that the use of the Duravev's approximation of the DFT+U always yields the first metastable state if the OM_F occupation matrix is not imposed at the beginning of the calculation. The Dudarev formalism is used by most authors who studied UO_2 within the DFT+U approximation, except Andersson *et al.*[11] who used the Liechtenstein approach. None of these authors, however, mentioned having controlled the occupation matrices. Consequently, it is very likely that their calculations yielded the first metastable state of the fluorite structure. This can be easily checked by looking at the cell parameters obtained, since in the fluorite structure, there is a dilatation along the c axis in the ground state while it is a compression in the metastable state. In the work of Iwasawa *et al.*,[6] Dorado *et al.*,[12] Gryaznov *et al.*,[17] and Yu *et al.*,[13] for instance, the slight compression along the c axis is observed. This means that the first metastable state was indeed reached. In the studies of Gupta *et al.*[7] and Nerikar *et al.*,[10] the cell is found to be perfectly cubic. We showed in Sec. III B 2 that the cubic cell can only be obtained without constraining symmetries by considering the noncollinear AFM order. We thus think that the cell was forced to remain cubic in these calculations but that the first metastable state was still reached. Consequently, all previous studies obtained very probably the same final state for the perfect supercell.

We present in Table XI the formation energy of the oxygen interstitial and vacancy given by the various authors, as well as our values for the fluorite structure. As already mentioned, there are large discrepancies in the formation energies published. The formation energy of a point defect involves three terms: the total energy of the perfect crystal, the total energy of the reference state for oxygen and the total energy of the defective supercell. We showed above that all previous studies had reached the same fluorite metastable state for the perfect crystal. In addition, the reference state for the oxygen atom is in all studies the dioxygen molecule calculated in the SP-GGA approximation and using the same PAW data sets. Any error in the total energy of the dioxygen molecule would only lead to a slight variation in the formation energies (less than 0.2 eV). The dioxygen molecule is therefore not the

TABLE XI. Formation energies of the oxygen interstitial and vacancy calculated by various authors using the Dudarev DFT+U approach.

	Iwasawa (Ref. [6])	Gupta (Ref. [7])	Nerikar (Ref. [10])	Dorado (Ref. [12])	Yu (Ref. [13])	This work
Relaxation	Complete	Volume only	Volume only	Complete	Volume only	Complete
Cut-off energy (eV)	400	400	400	400	500	500
GGA	PBE	PW91	PW91	PBE	PBE	PBE
I_O (eV)	−0.4	−1.6	−1.3		−2.44	0.10
V_O (eV)	4.5	5.6	5.3	3.5	5.06	5.67

origin of the discrepancies observed, contrary to the statement of Yu *et al.*[13] Consequently, the discrepancies must stem from the calculations of the defective supercells which reached different metastable states. In defective supercells, the number of metastable states increases significantly and the ground state is more difficult to reach, especially when symmetries are not switched off. Table VIII clearly points out this difficulty since each calculation reached a different state.

The error caused by considering the fluorite structure without imposing the ground-state occupation matrices significantly affects the formation energies published so far. We have indeed shown that the first metastable state is located 1.5 eV above the ground state (for the 96-atom supercell) and thus induces a significant underestimation of the formation energies. Consequently, to take this error into account, all formation energies found in the works cited above should be shifted upward by 1.5 eV. It could be argued that this error is also present in the calculations of defective supercells and therefore cancels out in the calculation of the formation energies. Our calculations show, however, that the error is much smaller in the calculations of point defects than in the perfect crystal, provided symmetries are switched off. In the particular case of Yu *et al.*,[13] it can be seen that their formation energy for the oxygen interstitial is largely negative. This low value stems from the fact that symmetries have probably been switched off in the calculations, and that the defective supercell converged toward the most stable phase at 0 K, e.g., a Jahn-Teller distorted structure. In the case of the oxygen vacancy, we had obtained the lowest formation energy published so far using SP-GGA wave functions as initial guess for the calculations.[12]

VI. CONCLUSION

In the present paper, we report DFT+U values of oxygen simple point defects in UO$_2$, both in the fluorite and the Jahn-Teller distorted structures. Contrary to previous studies, these values were calculated using an efficient occupation matrix control scheme which we developed on the perfect crystal. These are also the first DFT+U calculations in which the defects in the Jahn-Teller phase are considered. We first studied the Jahn-Teller distortion in perfect UO$_2$ in the noncollinear antiferromagnetic order. We show that the fluorite structure is not the most stable phase at 0 K, as seen experimentally. The most stable phase is a Jahn-Teller distorted structure that exhibits a distortion of the oxygen cage with an oxygen displacement along the $\langle 111 \rangle$ directions, in agreement with experiments. The oxygen displacement calculated is, however, larger than the experimental one. We show that this distortion of the oxygen cage stabilizes the structure by approximately 50 meV per uranium atom, which is a significant energy difference. As for the fluorite structure, we show that if occupation matrices are not controlled, the use of the Dudarev approach of the DFT+U systematically yields the first metastable state, which is located 45 meV per uranium atom above the fluorite ground state. This results in a large underestimation of the point-defect formation energies published in the literature. In the case of point-defect calculations, we confirm that occupation matrix control always allows one to reach the lowest energy states. Using this procedure, we find the formation energy of the single-oxygen interstitial to be 0.10 eV and 0.47 eV in the fluorite and the Jahn-Teller distorted structures, respectively. The extra oxygen atom induces a contraction of the cell parameters in good agreement with the experimental value. These are the first DFT+U calculations in which the formation energy of the single-oxygen interstitial is found to be positive. This is consistent with the experimental observations showing that UO$_{2+x}$ is not stable at 0 K. As concerns the oxygen vacancy, the formation energy is found to be 5.67 eV and 6.01 eV in the fluorite and the Jahn-Teller distorted structures, respectively. For oxygen simple point defects, the crystal field therefore seems to have only a moderate influence on the defect formation energies. Finally, we show that the discrepancies observed in the literature on the defect formation energies stem from the different metastable states of the defective supercells reached in the various calculations.

In the specific case of UO$_2$, the existence of the Jahn-Teller distortion facilitates the search of the lowest states due to the breaking in symmetries it induces. This is the reason why calculations without occupation matrix control reach low-energy states for oxygen point defects in the Jahn-Teller distorted structure. For direct comparisons of point-defect formation energies with experiments, however, the fluorite structure must be considered, and controlling occupation matrices is mandatory to reach the ground state. More generally, occupation matrices should always be controlled in studies using a method which localizes electrons, such as hybrid functionals, self-interaction correction method, or the DFT+U approximation.

ACKNOWLEDGMENTS

APPENDIX: OCCUPATION MATRICES

We report below the ground state and the first metastable state occupation matrices of bulk uranium dioxide in its fluorite structure, without taking into account the spin-orbit coupling. Occupation matrices are calculated in the basis of real spherical harmonics.

Within the Liechtenstein approach of the DFT+U, the occupation matrix is given by spin component ↑

$$
\begin{pmatrix}
0.347 & 0.000 & 0.450 & 0.000 & 0.000 & 0.000 & 0.000 \\
0.000 & 0.146 & 0.000 & 0.000 & 0.000 & 0.000 & 0.000 \\
0.450 & 0.000 & 0.677 & 0.000 & 0.000 & 0.000 & 0.000 \\
0.000 & 0.000 & 0.000 & 0.040 & 0.000 & 0.000 & 0.000 \\
0.000 & 0.000 & 0.000 & 0.000 & 0.677 & 0.000 & -0.450 \\
0.000 & 0.000 & 0.000 & 0.000 & 0.000 & 0.026 & 0.000 \\
0.000 & 0.000 & 0.000 & 0.000 & -0.450 & 0.000 & 0.347
\end{pmatrix}
$$

spin component ↓

$$
\begin{pmatrix}
0.033 & 0.000 & 0.002 & 0.000 & 0.000 & 0.000 & 0.000 \\
0.000 & 0.116 & 0.000 & 0.000 & 0.000 & 0.000 & 0.000 \\
0.002 & 0.000 & 0.025 & 0.000 & 0.000 & 0.000 & 0.000 \\
0.000 & 0.000 & 0.000 & 0.034 & 0.000 & 0.000 & 0.000 \\
0.000 & 0.000 & 0.000 & 0.000 & 0.025 & 0.000 & -0.002 \\
0.000 & 0.000 & 0.000 & 0.000 & 0.000 & 0.025 & 0.000 \\
0.000 & 0.000 & 0.000 & 0.000 & -0.002 & 0.000 & 0.033
\end{pmatrix}
$$

whereas in the first metastable state, it is given by spin component ↑

$$
\begin{pmatrix}
0.347 & 0.000 & -0.450 & 0.000 & 0.000 & 0.000 & 0.000 \\
0.000 & 0.146 & 0.000 & 0.000 & 0.000 & 0.000 & 0.000 \\
-0.450 & 0.000 & 0.677 & 0.000 & 0.000 & 0.000 & 0.000 \\
0.000 & 0.000 & 0.000 & 0.040 & 0.000 & 0.000 & 0.000 \\
0.000 & 0.000 & 0.000 & 0.000 & 0.677 & 0.000 & 0.450 \\
0.000 & 0.000 & 0.000 & 0.000 & 0.000 & 0.026 & 0.000 \\
0.000 & 0.000 & 0.000 & 0.000 & 0.450 & 0.000 & 0.347
\end{pmatrix}
$$

spin component ↓

$$
\begin{pmatrix}
0.033 & 0.000 & 0.002 & 0.000 & 0.000 & 0.000 & 0.000 \\
0.000 & 0.116 & 0.000 & 0.000 & 0.000 & 0.000 & 0.000 \\
0.002 & 0.000 & 0.025 & 0.000 & 0.000 & 0.000 & 0.000 \\
0.000 & 0.000 & 0.000 & 0.034 & 0.000 & 0.000 & 0.000 \\
0.000 & 0.000 & 0.000 & 0.000 & 0.025 & 0.000 & -0.002 \\
0.000 & 0.000 & 0.000 & 0.000 & 0.000 & 0.025 & 0.000 \\
0.000 & 0.000 & 0.000 & 0.000 & -0.002 & 0.000 & 0.033
\end{pmatrix} .
$$

[1] P. Hohenberg and W. Kohn, Phys. Rev. **136**, B864 (1964).

[2] W. Kohn and L. J. Sham, Phys. Rev. **140**, A1133 (1965).

[3] I. D. Prodan, G. E. Scuseria, and R. L. Martin, Phys. Rev. B **73**, 045104 (2006).

[4] L. Petit, A. Svane, Z. Szotek, and W. Temmerman, Science **301**, 498 (2003).

[5] S. L. Dudarev, G. A. Botton, S. Y. Savrasov, C. J. Humphreys, and A. P. Sutton, Phys. Rev. B **57**, 1505 (1998).

[6] M. Iwasawa, Y. Chen, Y. Kaneta, T. Ohnuma, H.-Y. Geng, and M. Kinoshita, Mater. Trans. **47**, 2651 (2006).

[7] F. Gupta, G. Brillant, and A. Pasturel, Philos. Mag. **87**, 2561 (2007).

[8] H. Y. Geng, Y. Chen, Y. Kaneta, M. Iwasawa, T. Ohnuma, and M. Kinoshita, Phys. Rev. B **77**, 104120 (2008).

[9] H. Y. Geng, Y. Chen, Y. Kaneta, and M. Kinoshita, Phys. Rev. B **77**, 180101(R) (2008).

[10] P. Nerikar, T. Watanabe, J. S. Tulenko, S. R. Phillpot, and S. B. Sinnott, J. Nucl. Mater. **384**, 61 (2009).

[11] D. A. Andersson, J. Lezama, B. P. Uberuaga, C. Deo, and S. D. Conradson, Phys. Rev. B **79**, 024110 (2009).

[12] B. Dorado, M. Freyss, and G. Martin, Eur. Phys. J. B **69**, 203 (2009).

[13] J. Yu, R. Devanathan, and W. J. Weber, J. Phys.: Condens. Matter **21**, 435401 (2009).

[14] G. Brillant and A. Pasturel, Phys. Rev. B **77**, 184110 (2008).

[15] G. Brillant, F. Gupta, and A. Pasturel, J. Phys.: Condens. Matter **21**, 285602 (2009).

[16] F. Gupta, A. Pasturel, and G. Brillant, J. Nucl. Mater. **385**, 368 (2009).

[17] D. Gryaznov, E. Heifets, and E. Kotomin, Phys. Chem. Chem. Phys. **11**, 7241 (2009).

[18] P. V. Nerikar, X.-Y. Liu, B. P. Uberuaga, C. R. Stanek, S. R. Phillpot, and S. B. Sinnott, J. Phys.: Condens. Matter **21**, 435602 (2009).

[19] B. Dorado, B. Amadon, M. Freyss, and M. Bertolus, Phys. Rev. B **79**, 235125 (2009).

[20] A. B. Shick, W. E. Pickett, and A. I. Lichtenstein, J. Electron Spectrosc. Relat. Phenom. **114-116**, 753 (2001).

[21] P. Larson, W. R. L. Lambrecht, A. Chantis, and M. van Schilfgaarde, Phys. Rev. B **75**, 045114 (2007).

[22] B. Amadon, F. Jollet, and M. Torrent, Phys. Rev. B **77**, 155104 (2008).

[23] G. Jomard, B. Amadon, F. Bottin, and M. Torrent, Phys. Rev. B **78**, 075125 (2008).

[24] F. Jollet, G. Jomard, B. Amadon, J. P. Crocombette, and D. Torumba, Phys. Rev. B **80**, 235109 (2009).

[25] F. Tran, J. Schweifer, P. Blaha, K. Schwarz, and P. Novák, Phys. Rev. B **77**, 085123 (2008).

[26] G. Kresse and J. Hafner, Phys. Rev. B **47**, 558 (1993).

[27] G. Kresse and J. Furthmüller, Comput. Mater. Sci. **6**, 15 (1996).

[28] G. Kresse and J. Furthmüller, Phys. Rev. B **54**, 11169 (1996).

[29] P. E. Blöchl, Phys. Rev. B **50**, 17953 (1994).

[30] G. Kresse and D. Joubert, Phys. Rev. B **59**, 1758 (1999).

[31] A. I. Liechtenstein, V. I. Anisimov, and J. Zaanen, Phys. Rev. B **52**, R5467 (1995).

[32] J. P. Perdew, K. Burke, and M. Ernzerhof, Phys. Rev. Lett. **77**, 3865 (1996).

[33] H. J. Monkhorst and J. D. Pack, Phys. Rev. B **13**, 5188 (1976).

[34] A. Kotani and T. Yamazaki, Prog. Theor. Phys. **108**, 117 (1992).

[35] R. Caciuffo, G. Amoretti, P. Santini, G. H. Lander, J. Kulda, and P. de V. Du Plessis, Phys. Rev. B **59**, 13892 (1999).

[36] D. Ippolito, L. Martinelli, and G. Bevilacqua, Phys. Rev. B **71**, 064419 (2005).

[37] E. Blackburn, R. Caciuffo, N. Magnani, P. Santini, P. J. Brown, M. Enderle, and G. H. Lander, Phys. Rev. B **72**, 184411 (2005).

[38] S. B. Wilkins, R. Caciuffo, C. Detlefs, J. Rebizant, E. Colineau, F. Wastin, and G. H. Lander, Phys. Rev. B **73**, 060406(R) (2006).

[39] P. Santini, S. Carretta, G. Amoretti, R. Caciuffo, N. Magnani, and G. H. Lander, Rev. Mod. Phys. **81**, 807 (2009).

[40] A. Georges, G. Kotliar, W. Krauth, and M. J. Rozenberg, Rev. Mod. Phys. **68**, 13 (1996).

[41] G. Kotliar, S. Y. Savrasov, K. Haule, V. S. Oudovenko, O. Parcollet, and C. A. Marianetti, Rev. Mod. Phys. **78**, 865 (2006).

[42] S. L. Dudarev, M. R. Castell, G. A. Botton, S. Y. Savrasov, C. Muggelberg, G. A. D. Briggs, A. P. Sutton, and D. Goddard, Micron **31**, 363 (2000).

[43] R. Laskowski, G. K. H. Madsen, P. Blaha, and K. Schwarz, Phys. Rev. B **69**, 140408(R) (2004).

[44] J. D. Higgs, W. T. Thompson, B. J. Lewis, and S. C. Vogel, J. Nucl. Mater. **366**, 297 (2007).

[45] E. R. Ylvisaker, W. E. Pickett, and K. Koepernik, Phys. Rev. B **79**, 035103 (2009).

[46] K. Teske, H. Ullmann, and D. Rettig, J. Nucl. Mater. **116**, 260 (1983).

[47] L. Van Brutzel, A. Chartier, and J. P. Crocombette, Phys. Rev. B **78**, 024111 (2008).